Angewandte Chemie
Eine Zeitschrift der Gesellschaft Deutscher Chemiker

Supporting Information

69451 Weinheim, Germany

Carbocation-Watching in Solvolysis Reactions

Heike F. Schaller and Herbert Mayr[a]*

[a] *Department Chemie und Biochemie*
Ludwig-Maximilians-Universität München
Butenandtstraße 5-13 (Haus F)
81377 München (Germany)
Fax: (+49) 89-2180-77717
E-mail: herbert.mayr@cup.uni-muenchen.de

General

Materials. Commercially available acetonitrile and water (HPLC-gradient grade, VWR) and acetone (extra dry, Acros) were used without further purification for all experiments.

Mixtures of solvents are given as (v/v) and the solvents are abbreviated: A = acetone, AN = acetonitrile, W = water. For example the solvent mixture 20W80AN refers to a mixture of water and acetonitrile in a ratio of 20/80 (v/v).

N,*N*-Diisopropylmethylamine ((*i*Pr)$_2$NMe, ≥ 98 %, Fluka) was distilled, quinuclidine (≥ 97 %, Fluka) and 4-(dimethylamino)pyridine (DMAP, > 99 %, Aldrich) were used without further purification.

The benzhydrylium tetrafluoroborates Ar_2CH^+ BF_4^- were prepared as described before.[S1]

The covalent benzhydryl carboxylates **1-PNB** and **2-PNB** which are derived from highly stabilized benzhydrylium ions (**1**$^+$ and **2**$^+$) and good nucleofuges (PNB$^-$) cannot be isolated.

*4,4'-Bis(morpholino)benzhydryl acetate (**1-OAc**)*. A mixture of 4,4'-bis(morpholino)benzhydrol (354 mg, 1.0 mmol), DMAP (0.1 equiv, 12 mg, 0.10 mmol), and freshly distilled triethylamine (1.2 equiv, 101 mg, 1.00 mmol) in dry benzene (5 mL) was stirred for 5 min under nitrogen atmosphere before acetic anhydride (1 equiv) was added. Stirring was continued for 5 h at room temperature. Then pentane (5 mL) was added, and the reaction mixture was washed quickly with 0.2 M hydrochloric acid (10 mL), saturated aq. $NaHCO_3$ (10 mL), and water. The organic phase was dried ($MgSO_4$) and filtered. Then the solvent was evaporated in vacuo (< 30°C). The residue was crystallized from diethyl ether/pentane to give **1-OAc** (258 mg, 65%) as a colorless powder.

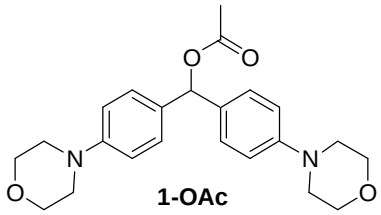

1-OAc

^{1}H NMR (200 MHz, C_6D_6): δ = 1.73 (s, 3 H, CH_3), 2.65 (pretended t, 8 H, *J* = 3.5 Hz, NCH_2), 3.46 (pretended t, 8 H, *J* = 3.5 Hz, OCH_2), 6.63 (d, 4H, *J* = 8.7 Hz, ArH), 7.21 (s, 1 H, Ar_2CH), 7.38 ppm (d, 4 H, *J* = 8.7 Hz, ArH); ^{13}C NMR (75.5 MHz, C_6D_6): δ = 21.3 (q, CH_3), 49.6 (t, NCH_2), 67.2 (t, OCH_2), 77.2 (d, Ar_2CH), 116.1 (d, Ar), 129.1 (d, Ar), 132.9 (s, Ar), 151.7 (s, Ar), 169.9 ppm (s, CO_2).

[S1] H. Mayr, T. Bug, M. F. Gotta, N. Hering, B. Irrgang, B. Janker, B. Kempf, R. Loos, A. R. Ofial, G. Remennikov, H. Schimmel, *J. Am. Chem. Soc.* **2001**, *123*, 9500–9512.

Kinetics

Solvolysis Reactions by Conductometry. For the conductometric monitoring of the solvolysis reactions of **1-OAc** in 20W80AN a WTW LTA 1/NS Pt electrode connected to a Tacussel CD 810 conductometer was used.[S2] To freshly prepared aqueous solvent mixtures (20W80AN, 25 mL) amine was added and the mixtures were thermostated (25.0 ± 0.1 °C) prior to the injection of a small volume (75–150 µL) of a 0.2 M stock solution of **1-OAc** in CH_2Cl_2. The increase of the conductance (*G*) was then recorded.

Solvolysis Reactions by Conventional UV-Vis-Photometry. For the UV-Vis-photometric investigation of the solvolysis reactions of **1-OAc** in 20W80AN a conventional UV-Vis-photometry setup was used (J&M TIDAS diode array spectrophotometer connected through fiber optic cables with standard SMA connectors to a Hellma 661.060-UV quartz Suprasil immersion probe with 5 mm light path). To freshly prepared aqueous solvent mixtures (20W80AN, 25 mL) a specific amount of amine was added and the mixtures were thermostated (25.0 ± 0.1 °C) prior to the injection of a small volume (75–150 µL) of a stock solution of **1-OAc** in CH_2Cl_2.

Solvolysis Reactions by Stopped-Flow UV-Vis-Photometry. The covalent benzhydryl carboxylates **1-PNB** and **2-PNB**, which are derived from highly stabilized benzhydrylium ions (**1**$^+$ and **2**$^+$) and good nucleofuges (PNB^-), cannot be isolated. Therefore the double mixing mode of a stopped-flow instrument (Hi-Tech SF-61DX2 controlled by Hi-Tech KinetAsyst3 software) was employed to generate the covalent benzhydryl esters by first mixing a solution of $Ar_2CH^+BF_4^-$ in acetone with a solution of 10 to 80 equiv. of *n*-$Bu_4N^+PNB^-$ in the same solvent. After a delay time of 1 s, the colorless solution of the resulting covalent Ar_2CH-PNB was combined in a second mixing step with an equal volume of *aqueous* acetone, which provoked the ionization of Ar_2CH–PNB. The ionizations were followed photometrically at the absorption maxima of Ar_2CH^+. The concentrations of the generated benzhydrylium carboxylates were between (2.5...10) × 10^{-6} mol L^{-1}. The excess of carboxylate ions varied between 10 and 80 equiv. of the Ar_2CH-PNB.

Evaluation of Kinetic Measurement by GEPASI software. Whenever we were not able to analyze the kinetic traces by a fit to a single-exponential function, we used the "evolutionary programming" optimization method implemented in the GEPASI software (version 3.30)[S3] to calculate the rate constants k_1, k_{-1}, and k_{Solv}.

For this procedure the experimentally measured time-dependent conductance or absorption curves must be converted to concentration vs time curves. In case of the conductometric measurements, a calibration curve for *n*-$Bu_4N^+AcO^-$ in 20W80AN was used for this conversion. Differences of the specific conductivities of Ar_2CH^+, R_3NH^+, and R_4N^+ have been neglected.

[S2] H. Mayr, R. Schneider, C. Schade, J. Bartl, R. Bederke, *J. Am. Chem. Soc.* **1990**, *112*, 4446–4454.

[S3] a) P. Mendes, *Comput. Appl. Biosci.* **1993**, *9*, 563–571; b) P. Mendes, *Trends Biochem. Sci.* **1997**, *22*, 361–363; c) P. Mendes, D. Kell, *Bioinformatics* **1998**, *14*, 869–883; d) More information about GEPASI at: www.gepasi.org.

Absorptions were converted to the corresponding concentrations of Ar_2CH^+ by using the absorption coefficients.[S4]

Besides the experimentally obtained kinetic curves (conc vs time), a set of equations (see below) that describes a simple S_N1 solvolysis reaction (Scheme 1, main article) was used as input for the GEPASI software. Then, the "evolutionary programming" method of GEPASI searches for a global minimum of the sum of squares of residuals *ssq* (eq (S1)) of the adjustable variables (= rate constants k_1, k_{-1}, and k_{Solv}), the experimental kinetic curves, and the initial concentrations of the involved species.

$$ssq = \sum_i \left(\frac{y_i - y_i^*}{w_i} \right)^2 \qquad \text{eq (S1)}$$

In Equation (S1), y_i are the measured values of the variables, y^*_i are the simulated values of the variables and w_i are weighting constants. The weighting constants are used to scale all variables to similar values so that they have equal weight on the fit. The smaller *ssq*, the better the fit.

[S4] R. Loos, H. Mayr, unpulished results.

Conductimetric Investigation of the Solvolysis Reactions of 1-OAc in 20W80AN in Presence of Different Amines

The solvolysis reactions of **1-OAc** in 20W80AN (at 25 °C) were monitored by following the increase of the conductivity of the reaction mixtures.

In the presence of added DMAP or quinuclidine (Scheme 3), the first-order rate constants k_1 (s^{-1}) for the solvolysis reactions of **1-OAc** were obtained by least-squares fitting of the single exponential equation $y = A_1\exp(-x/t_1) + y_0$ (with $1/t_1 = k_1$) to the conductance data (Figures S1 and S2).

In presence of diisopropyl-methylamine ((*i*Pr)$_2$NMe), however, the increase of conductivity during the solvolysis reaction of **1-OAc** in 20W80AN cannot be described by a single exponential function (Figure S3) and a fit calculated by GEPASI according to Scheme 1 was applied to analyze the kinetics (Figure S4).

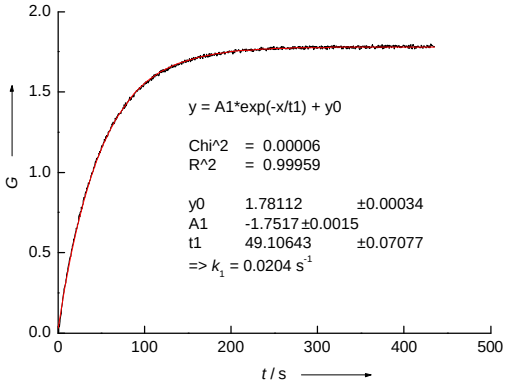

Figure S1. Increase of conductivity during the solvolysis of **1-OAc** (0.622 mM) in 20W80AN at 25 °C in the presence of DMAP (5.02 mM). Superposition of experimental curve (black) and exponential fit (red).

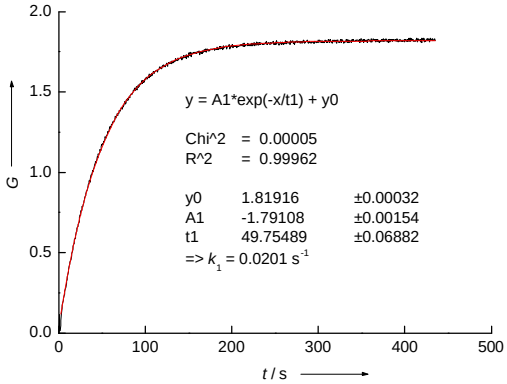

Figure S2. Increase of conductivity during the solvolysis of **1-OAc** (0.622 mM) in 20W80AN at 25 °C in the presence of quinuclidine (5.24 mM). Superposition of experimental curve (black) and exponential fit (red).

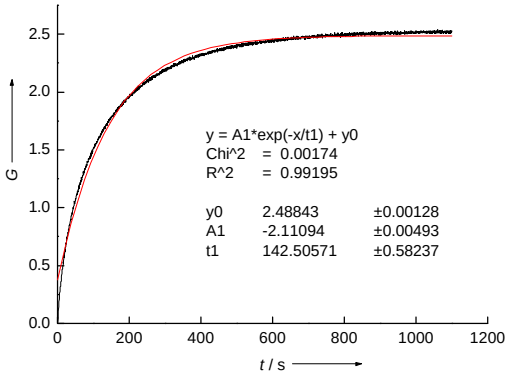

Figure S3. Increase of conductivity during the solvolysis of **1-OAc** (0681 mM) in 20W80AN at 25 °C in the presence of (*i*Pr)$_2$NMe (5.24 mM). The superposition of experimental curve (black) and exponential fit (red) shows systematic deviations.

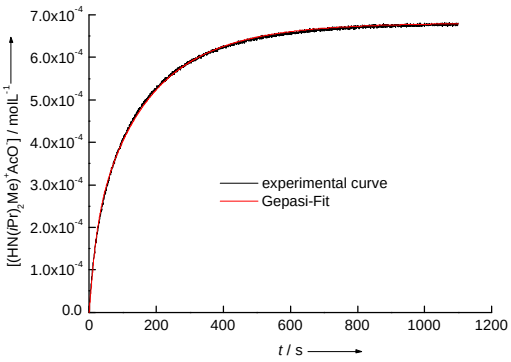

Figure S4. Increase of conductivity during the solvolysis of **1-OAc** (0.681 mM) in 20W80AN at 25 °C in the presence of (*i*Pr)$_2$NMe (0.524 mM). The superposition of experimental curve (black) and a fit calculated by GEPASI (red, *ssq* = 1.04 × 10^{-8}) according to Scheme 1 delivers the rate constants:
k_1 = (2.13 ± 0.00) × 10^{-2} s^{-1};
k_{-1} = (1.09 ± 0.04) × 10^3 M^{-1} s^{-1};
k_{Solv} = (2.01 ± 0.07) × 10^{-1} s^{-1}.

Photometric Investigation of the Solvolysis Reaction of 1-OAc in 20W80AN

The solvolysis reactions of **1-OAc** in 20W80AN (at 25 °C) were monitored by conventional UV-Vis-photometry. The increase and subsequent decay of the absorbance at 612 nm (Figure S5) was used for the GEPASI analysis of the kinetics of the solvolysis reaction according to Scheme 1.

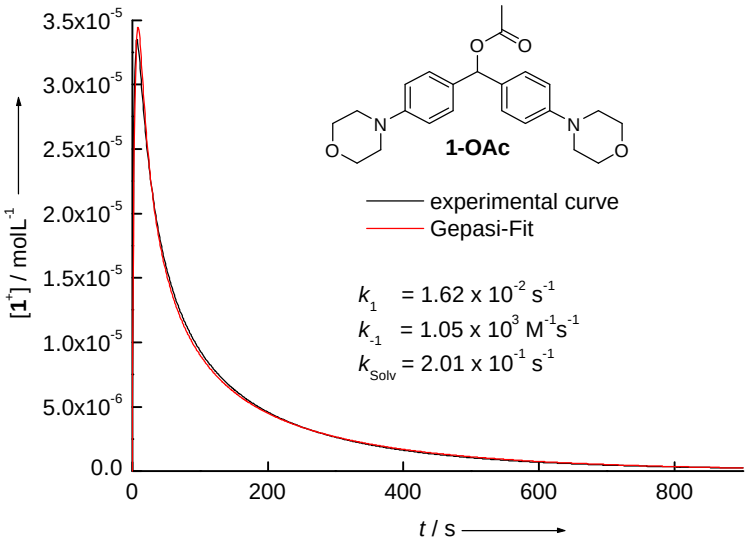

Figure S5. Formation and consumption of the blue carbocation $\mathbf{1}^+$ (monitored at 612 nm, conventional UV-Vis-photometry, absorptions are converted to concentrations of $\mathbf{1}^+$) during the heterolysis of **1-OAc** (1.09 mM) in 20W80AN at 25 °C in the presence of $(i\text{Pr})_2\text{NMe}$ (5.24 mM). The superposition of experimental curve (black) and a fit calculated by GEPASI (red, *ssq* = 1.33×10^{-10}) according to Scheme 1 delivers the rate constants: $k_1 = (1.62 \pm 0.00) \times 10^{-2}$ s^{-1}; $k_{-1} = (1.05 \pm 0.04) \times 10^{3}$ M^{-1} s^{-1}; $k_{Solv} = (2.01 \pm 0.07) \times 10^{-1}$ s^{-1} (Figure 1 of main article).

Without added $(i\text{Pr})_2\text{NMe}$, the solvolysis reaction **1-OAc** in 20W80AN (Figure S6) could not be analyzed by GEPASI within the framework of Scheme 1, probably because of the involvement of several rate and equilibrium constants (partial dissociation of acetic acid).

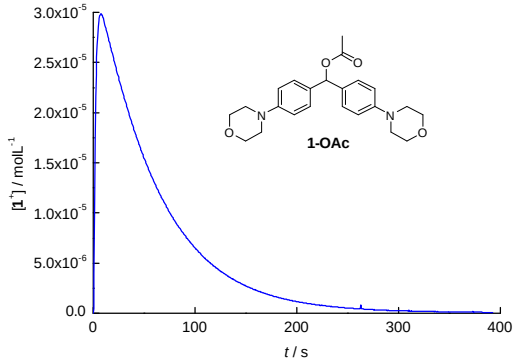

Figure S6. Formation and consumption of the blue carbocation $\mathbf{1}^+$ (monitored at 612 nm, conventional UV-Vis-photometry, absorptions are converted to concentrations of $\mathbf{1}^+$) during the heterolysis of **1-OAc** (0.908 mM) in 20W80AN at 25 °C.

Photometric Investigation of the Solvolysis Reactions of 1-PNB in 20W80A

The solvolysis reactions of **1-PNB** in 20W80A (at 25 °C) were monitored by stopped-flow UV-Vis-photometry. The increase and subsequent decay of the absorbance at 612 nm (Figure S7) was used for the GEPASI analysis of the kinetics of the solvolysis reaction according to Scheme 1 (Table S1).

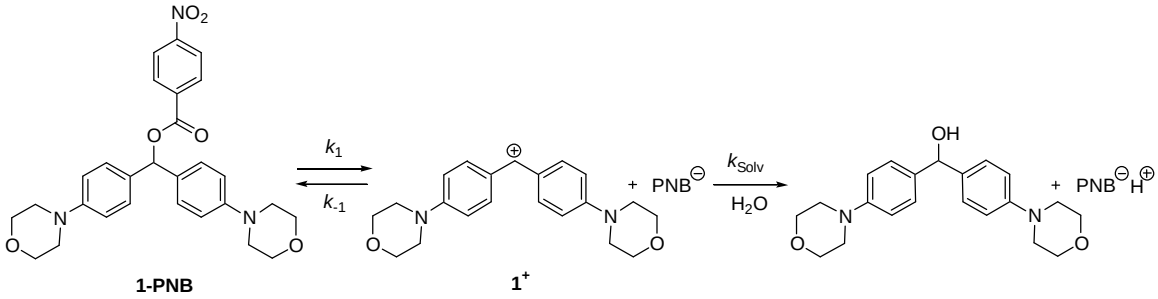

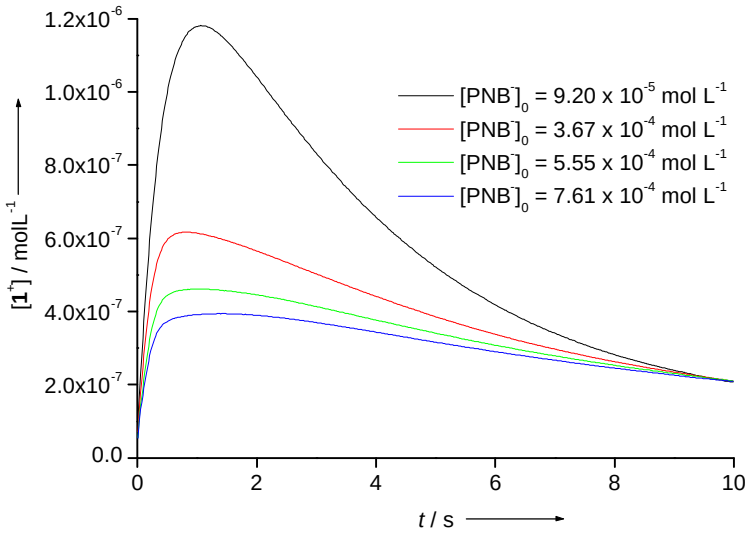

Figure S7. Formation and consumption of the blue carbocation $\mathbf{1}^+$ (monitored at 612 nm, stopped-flow technique, absorptions are converted to concentrations of $\mathbf{1}^+$) during the heterolysis of **1-PNB** (1.04×10^{-5} M) in 20W80A at 25 °C in the presence of different amounts of $n\mathrm{Bu_4N^+PNB^-}$ (Figure 3 of main article).

Table S1. Variation of the *p*-nitrobenzoate concentration and effect on the rate constants k_1, k_{-1}, and k_{Solv} (obtained from an analysis of the kinetic curves shown in Figure S7 by GEPASI) of the solvolysis reactions of **1-PNB** in 20W80A at 25 °C.

$[\mathbf{1\text{-}PNB}]_0$ [M]	$[PNB^-]_0$ [M]	k_1 [s^{-1}]	k_{-1} [M^{-1} s^{-1}]	k_{Solv} [s^{-1}]	*ssq*
1.04×10^{-5}	9.20×10^{-5}	-	-	-	-
1.04×10^{-5}	3.67×10^{-4}	$(2.57 \pm 0.00) \times 10^{-1}$	$(5.80 \pm 0.05) \times 10^{3}$	1.53 ± 0.00	2.07×10^{-14}
1.04×10^{-5}	5.55×10^{-4}	$(1.92 \pm 0.00) \times 10^{-1}$	$(4.00 \pm 0.05) \times 10^{3}$	1.50 ± 0.00	3.14×10^{-14}
1.04×10^{-5}	7.61×10^{-4}	$(1.61 \pm 0.00) \times 10^{-1}$	$(2.98 \pm 0.05) \times 10^{3}$	1.43 ± 0.00	4.22×10^{-14}

Photometric Investigation of the Solvolysis Reactions of 1-PNB in 40W60A

The solvolysis reactions of **1-PNB** in 40W60A (at 25 °C) were monitored by stopped-flow UV-Vis-photometry. The increase and subsequent decay of the absorbance at 612 nm (Figure S8) was used for the GEPASI analysis of the kinetics of the solvolysis reaction according to Scheme 1 (Table S2).

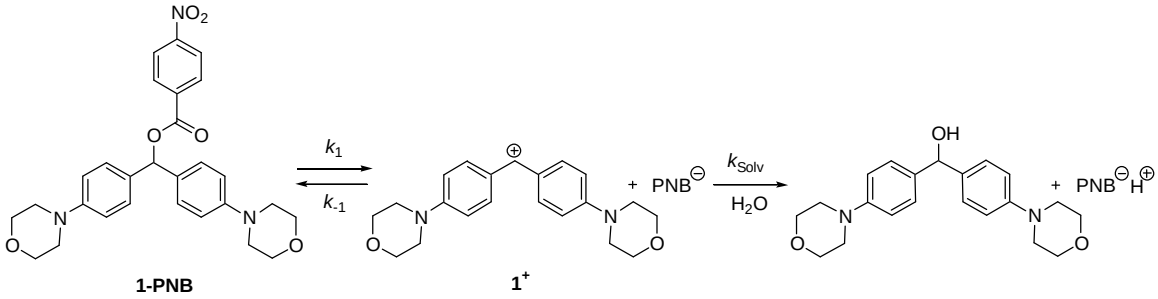

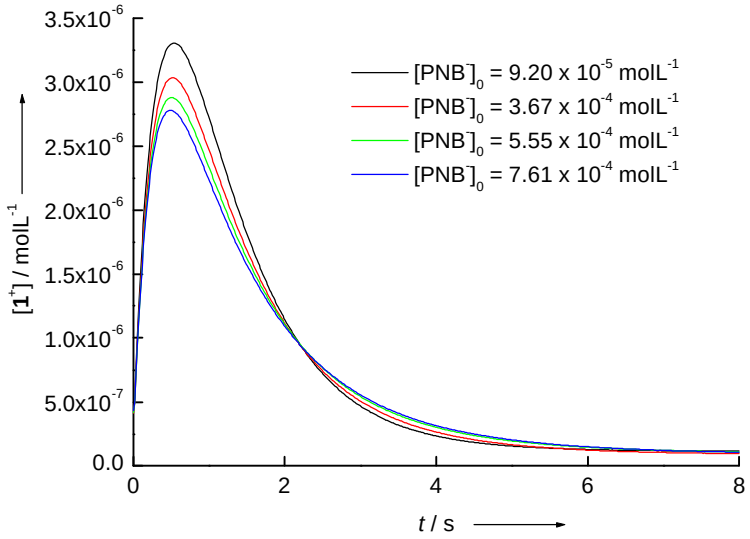

Figure S8. Formation and consumption of the blue carbocation **1**$^+$ (monitored at 612 nm, stopped-flow technique, absorptions are converted to concentrations of **1**$^+$) during the heterolysis of **1-PNB** (1.04×10^{-5} M) in 40W60A at 25 °C in the presence of different amounts of nBu$_4$N$^+$PNB$^-$ (Figure 4 of main article).

Table S2. Variation of the *p*-nitrobenzoate concentration and effect on the rate constants k_1, k_{-1}, and k_{Solv} (obtained from an analysis of the kinetic curves shown in Figure S8 by GEPASI) of the solvolysis reactions of **1-PNB** in 40W60A at 25 °C.

[**1-PNB**]$_0$ [M]	[PNB$^-$]$_0$ [M]	k_1 [s^{-1}]	k_{-1} [M^{-1} s^{-1}]	k_{Solv} [s^{-1}]	*ssq*
1.04×10^{-5}	9.20×10^{-5}	-	-	-	-
1.04×10^{-5}	3.67×10^{-4}	1.79 ± 0.01	$(3.63 \pm 0.06) \times 10^3$	1.81 ± 0.00	1.49×10^{-12}
1.04×10^{-5}	5.55×10^{-4}	1.79 ± 0.00	$(3.10 \pm 0.05) \times 10^3$	1.81 ± 0.00	1.74×10^{-12}
1.04×10^{-5}	7.61×10^{-4}	1.81 ± 0.01	$(2.62 \pm 0.04) \times 10^3$	1.84 ± 0.00	1.58×10^{-12}

Photometric Investigation of the Solvolysis Reactions of 2-PNB in 20W80A

The solvolysis reactions of **2-PNB** in 20W80A (at 25 °C) were monitored by stopped-flow UV-Vis-photometry. The increase and subsequent decay of the absorbance at 613 nm (Figure S9) was used for the GEPASI analysis of the kinetics of the solvolysis reaction according to Scheme 1 (Table S3).

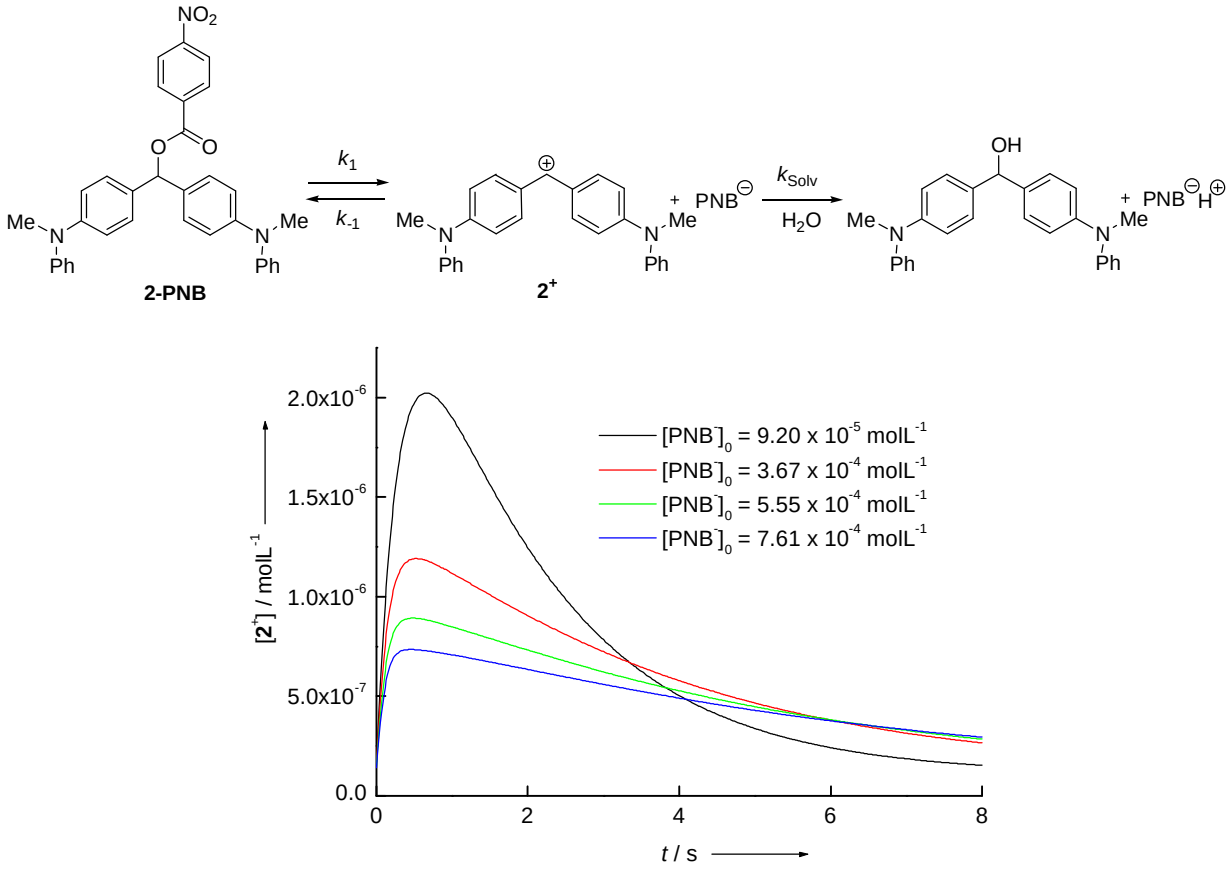

Figure S9. Formation and consumption of the blue carbocation **2**$^+$ (monitored at 613 nm, stopped-flow technique, absorptions are converted to concentrations of **2**$^+$) during the heterolysis of **2-PNB** (9.48 × 10^{-6} M) in 20W80A at 25 °C in the presence of different amounts of nBu$_4$N$^+$PNB$^-$.

Table S3. Variation of the *p*-nitrobenzoate concentration and effect on the rate constants k_1, k_{-1}, and k_{Solv} (obtained from an analysis of the kinetic curves shown in Figure S9 by GEPASI) of the solvolysis reactions of **2-PNB** in 20W80A at 25 °C.

[**2-PNB**]$_0$ [M]	[PNB$^-$]$_0$ [M]	k_1 [s^{-1}]	k_{-1} [M^{-1} s^{-1}]	k_{Solv} [s^{-1}]	*ssq*
9.48 × 10^{-6}	9.33 × 10^{-5}	1.08 ± 0.00	(1.69 ± 0.02) × 10^4	1.55 ± 0.00	3.39 × 10^{-13}
9.48 × 10^{-6}	3.67 × 10^{-4}	1.00 ± 0.00	(1.30 ± 0.00) × 10^4	1.51 ± 0.00	4.41 × 10^{-14}
9.48 × 10^{-6}	5.55 × 10^{-4}	(9.08 ± 0.04) × 10^{-1}	(1.17 ± 0.06) × 10^4	1.53 ± 0.00	2.74 × 10^{-14}
9.48 × 10^{-6}	7.61 × 10^{-4}	(8.47 ± 0.05) × 10^{-1}	(1.04 ± 0.00) × 10^4	1.49 ± 0.00	3.12 × 10^{-14}

Photometric Investigation of the Solvolysis Reactions of 2-PNB in 40W60A

The solvolysis reactions of **2-PNB** in 40W60A (at 25 °C) were monitored by stopped-flow UV-Vis-photometry. The increase and subsequent decay of the absorbance at 613 nm (Figure S10) was used for the GEPASI analysis of the kinetics of the solvolysis reaction according to Scheme 1 (Table S4).

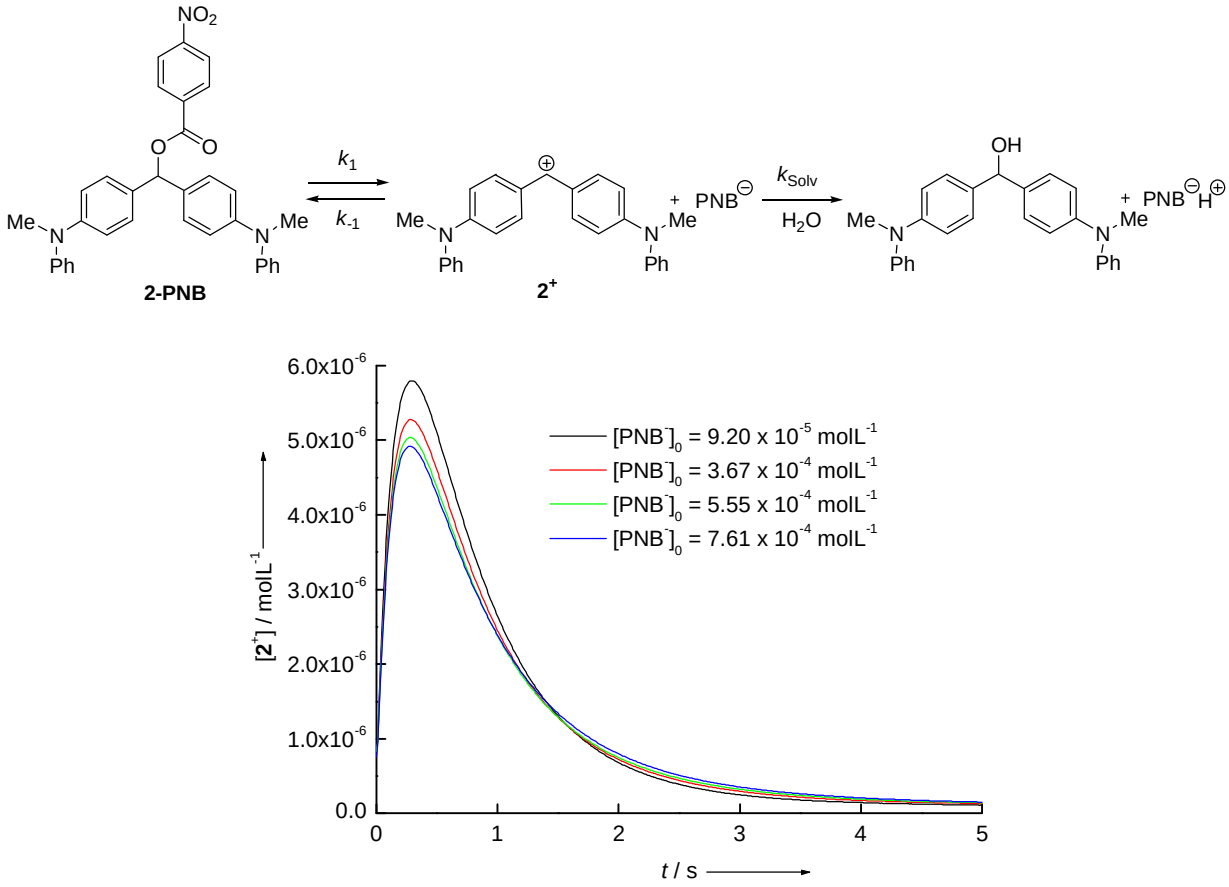

Figure S10. Formation and consumption of the blue carbocation **2**$^+$ (monitored at 613 nm, stopped-flow technique, absorptions are converted to concentrations of **2**$^+$) during the heterolysis of **2-PNB** (9.48×10^{-6} M) in 40W60A at 25 °C in the presence of different amounts of nBu$_4$N$^+$PNB$^-$.

Table S4. Variation of the *p*-nitrobenzoate concentration and effect on the rate constants k_1, k_{-1}, and k_{Solv} (obtained from an analysis of the kinetic curves shown in Figure S10 by GEPASI) of the solvolysis reactions of **2-PNB** in 40W60A at 25 °C.

[**2-PNB**]$_0$ [M]	[PNB$^-$]$_0$ [M]	k_1 [s^{-1}]	k_{-1} [M^{-1} s^{-1}]	k_{Solv} [s^{-1}]	*ssq*
9.48×10^{-6}	9.33×10^{-5}	6.57 ± 0.03	(5.76 ± 0.17) × 10^3	1.51 ± 0.00	2.83×10^{-12}
9.48×10^{-6}	3.67×10^{-4}	6.36 ± 0.04	(3.96 ± 0.07) × 10^3	1.59 ± 0.00	3.66×10^{-12}
9.48×10^{-6}	5.55×10^{-4}	6.30 ± 0.00	(3.56 ± 0.06) × 10^3	1.62 ± 0.00	4.07×10^{-12}
9.48×10^{-6}	7.61×10^{-4}	6.28 ± 0.04	(3.08 ± 0.05) × 10^3	1.60 ± 0.00	4.00×10^{-12}